

Emerging Photoluminescence in Monolayer MoS₂

Andrea Splendiani, †,† Liang Sun, † Yuanbo Zhang, † Tianshu Li, § Jonghwan Kim, † Chi-Yung Chim, † Giulia Galli, § and Feng Wang* $^{*,\dagger,\parallel}$

†Physics Department, University of California at Berkeley, Berkeley, California 94720, †Scuola Galileiana di Studi Superiori di Padova, 35122 Padova, Italy, §Chemistry Department, University of California at Davis, Davis, California 95616, and Materials Science Division, Lawrence Berkeley National Laboratory, Berkeley, California 94720

ABSTRACT Novel physical phenomena can emerge in low-dimensional nanomaterials. Bulk MoS₂, a prototypical metal dichalcogenide, is an indirect bandgap semiconductor with negligible photoluminescence. When the MoS₂ crystal is thinned to monolayer, however, a strong photoluminescence emerges, indicating an indirect to direct bandgap transition in this d-electron system. This observation shows that quantum confinement in layered d-electron materials like MoS₂ provides new opportunities for engineering the electronic structure of matter at the nanoscale.

KEYWORDS Photoluminescence, two-dimensional materials, metal dichalcogenide

ecent advances in fabrication of ultrathin layered materials down to unit cell thickness (monolayers)¹ have enabled explorations of new low-dimensional physics, as exemplified by massless Dirac fermions and anomalous quantum Hall effects observed in monolayer graphene.^{2,3} Layered transition metal dichalcogenides represent another class of materials, in which d-electrons' interactions can give rise to new physical phenomena.^{4,5} MoS₂ is a prototypical transition metal chalcogenide material. It is composed of covalently bonded S-Mo-S sheets that are bound by weak van der Waals forces. In its bulk form, MoS₂ is a semiconductor with an indirect bandgap of about 1 eV^{6,7} and it has been exploited for photovoltaic⁶ and photocatalytic⁷ applications due to its strong absorption in the solar spectrum region. Quantum confinement effects on the electronic structure and optical properties of MoS₂ have been previously observed in MoS2 thin films^{8,9} as well as in MoS_2 nanoplates 10 and nanotubes. 11 However, little is known about the properties of extended two-dimensional MoS₂ sheets down to unit cell thickness.

Here we report the emergence of photoluminescence in ultrathin layers of MoS_2 . We found that MoS_2 photoluminescence, surprisingly, increases with decreasing layer thickness, and that luminescence from a monolayer is the strongest while it is absent in bulk material. This unusual luminescence behavior is in accord with a recent theoretical prediction; MoS_2 , an indirect bandgap material in its bulk form, becomes a direct bandgap semiconductor when thinned to a monolayer. Our results demonstrate that quantum confinement in layered d-electron materials have

manifestations drastically different from those found in spbonded semiconductor nanostructures.

Ultrathin MoS₂ layers were fabricated using microexfoliation techniques on both quartz and Si/SiO2 wafers following the prescription of ref 1. Few-layer MoS₂ flakes were first identified by optical contrast in a microscope. Figure 1 a displays an optical microscope image of a typical ultrathin MoS₂ sample on Si/SiO₂ substrate. The silicon wafer with 280 nm thermal SiO₂ is represented by the purple-colored background, and regions with different shades of blue correspond to MoS₂ layers of different thicknesses. Comparisons between the observed optical contrast and theoretical estimates indicate that region "1L" is covered by a monolayer of MoS₂. This identification is confirmed by atomic force microscopy (AFM) images of the same sample (Figure 1b); the average step height from the substrate to flake "1L" is measured to be 0.7 nm and agrees well with the monolayer thickness of 0.6 nm for S-Mo-S structures. 12 Similarly, we were able to identify region "2L", "4L", and "6L" as bilayer, quadrilayer, and hexalayer MoS2, respectively (Figure 1c). For few-layer MoS₂ crystals on quartz substrate, we relied on optical contrast for estimation of the layer thickness.

We investigated optical properties in few-layer MoS $_2$ structures through optical reflection, Raman scattering, and photoluminescence spectroscopy. All the spectroscopy measurements were carried out in a confocal microscopy setup in which we can readily locate and selectively excite MoS $_2$ flakes of different layer thicknesses. Spatial resolution of the microscopy system is $\sim 1~\mu m$. In reflection spectroscopy, we employed a supercontinuum laser source (Fianium SC-450) to probe MoS $_2$ samples on the quartz substrate. For Raman scattering and photoluminescence measurements, we used a 532 nm solid state laser to excite few-layers MoS $_2$ on a Si/

Received for review: 11/18/2009 Published on Web: 03/15/2010



 $[\]mbox{\ensuremath{^{\ast}}}$ To whom correspondence should be addressed. E-mail: fengwang 76@ berkeley edu.



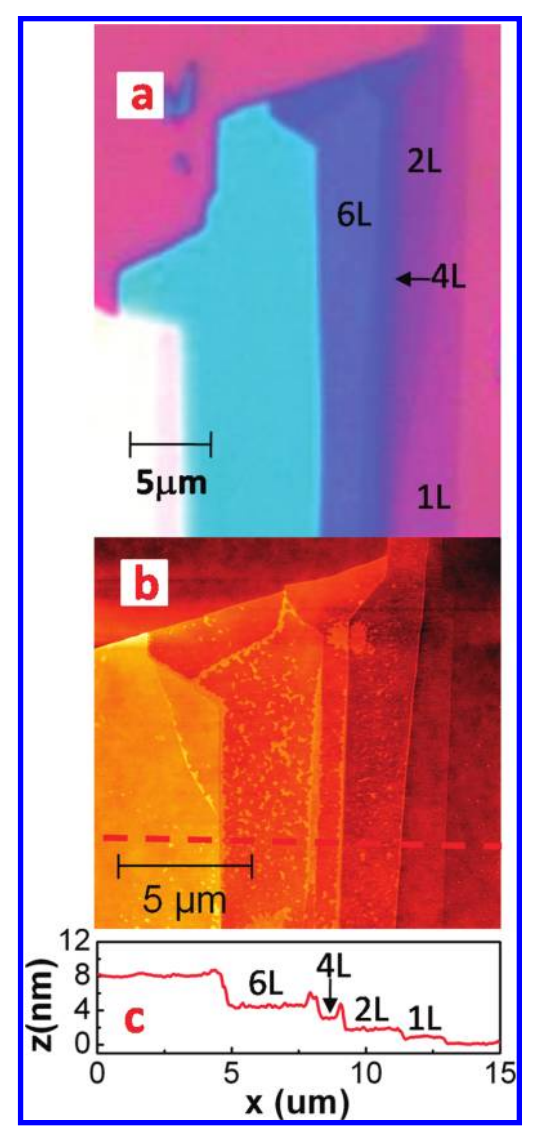


FIGURE 1. Exfoliated MoS_2 flakes on a Si/SiO_2 substrate. (a) Optical microscope image of the exfoliated MoS_2 sample. The purple background is from the Si/SiO_2 substrate and areas with different contrast correspond to MoS_2 flakes of different thicknesses. On the basis of the contrast, we infer areas labeled as "1L", "2L", and "4L" to be monolayer, bilayer, and quadrilayer, respectively. (b) Atomic force microscope (AFM) image of the same sample. (c) Sample height along the red line in b, which confirms the optical determined thicknesses of areas 1L, 2L, and 4L. It also shows area 6L to be a hexalayer.

 ${\rm SiO_2}$ wafer. In both cases, the spectra were recorded by a spectrometer equipped with a liquid nitrogen cooled camera.

We first determine the optical transitions in few-layer MoS_2 samples using reflection spectroscopy in a microscopy setup. Reflectivity differences between the bare quartz substrate and regions with ultrathin MoS_2 layers were measured across the visible and near IR spectral range (Figure 2a). For ultrathin layers of MoS_2 , the difference in reflectivity is directly proportional to the absorption constant. Two prominent absorption peaks can be identified at 670 and 627 nm in the spectrum. These two resonances have been well established to be the direct excitonic transitions (Figure

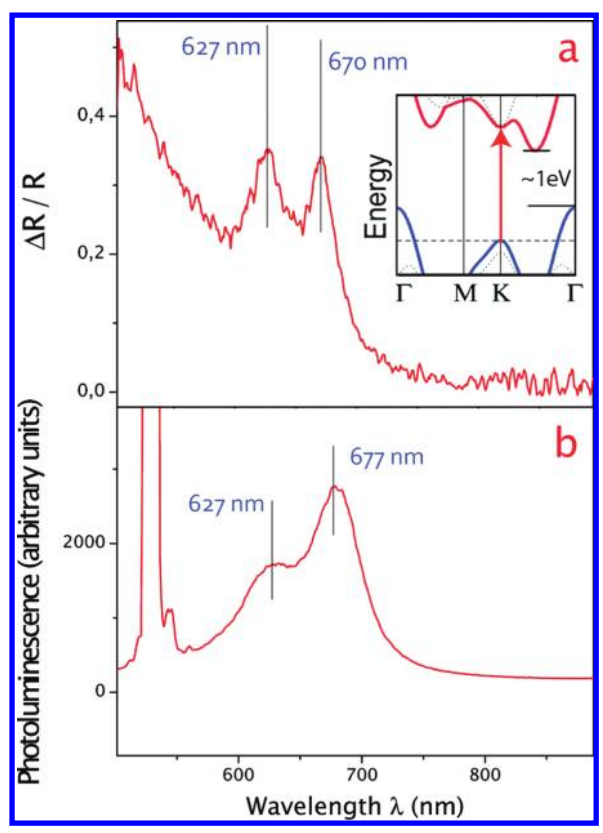


FIGURE 2. Reflection and photoluminescence spectra of ultrathin MoS_2 layers. (a) Reflection difference due to an ultrathin MoS_2 layer on a quartz substrate, which is proportional to the MoS_2 absorption constant. The observed absorption peaks at 1.85 eV (670 nm) and 1.98 eV (627 nm) correspond to the A1 and B1 direct excitonic transitions with the energy split from valence band spin—orbital coupling. The inset shows the bulk MoS_2 band structure neglecting the relatively weak spin—orbital coupling, which has an indirect bandgap around 1 eV and a single higher energy direct excitonic transition at the K point denoted by an arrow. (b) A strong photoluminescence is observed at the direct excitonic transitions energies in a monolayer MoS_2 . Such luminescence is absent in the indirect bandgap bulk MoS_2 sample.

2a inset) at the Brillouin zone K point. Their energy difference is due to the spin—orbital splitting of the valence band (not included in the calculation of Figure 2a inset), and the two resonances are known as A1 and B1 excitons, respectively. 14,15 (The strong peak at 532 nm is the elastic scattered laser radiation.) Optical absorption at energies between the direct excitonic transitions and the indirect bandgap (\sim 1 eV) is very weak. For thin layers of MoS₂, absorption peaks from the direct excitonic states exhibit little change with layer thicknesses.

Photoluminescence, however, exhibits a very different behavior. Figure 2b displays a photoluminescence spectrum of a monolayer MoS_2 . Pronounced luminescence emissions are observed at the A1 and B1 direct excitonic transitions. This photoluminescence emission in monolayer is in striking contrast to its absence in bulk MoS_2 , a consequence of bulk MoS_2 being an indirect bandgap semiconductor like silicon. In Figure 3a, we examine in more detail photoluminescence spectra from monolayer, bilayer, hexalayer, and bulk MoS_2



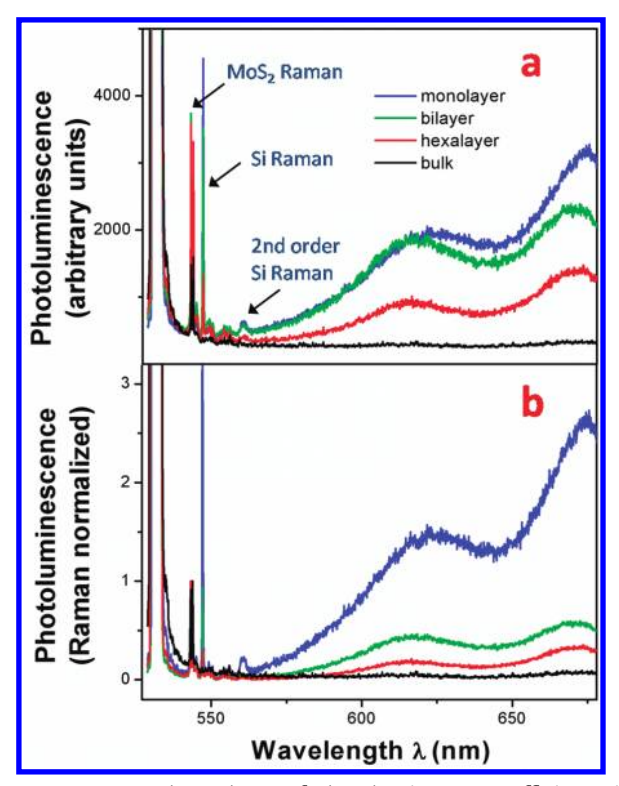


FIGURE 3. Layer dependence of photoluminescence efficiency in MoS_2 . (a) Photoluminescence and Raman spectra of MoS_2 monolayer, bilayer, hexalayer, and bulk sample. Different Raman peaks can be assigned to the MoS_2 and silicon vibration modes. For MoS_2 thin layers, monolayer MoS_2 Raman signal is relatively weak because less material is being excited. However, photoluminescence is the strongest in monolayer MoS_2 in spite of reduced material. (b) Photoluminescence spectra normalized by Raman intensity for MoS_2 layers with different thickness, showing a dramatic increase of luminescence efficiency in MoS_2 monolayer.

(in the form of very thick flakes). In addition to the relatively broad photoluminescence, three prominent Raman modes can be identified in the spectra: the first peak corresponds to a MoS₂ Raman excitation with a 408 cm⁻¹ Raman shift¹² and the next two at 520 and 1030 cm⁻¹ are the first and second order Raman peaks from the silicon substrate. 16 In bulk MoS₂, no photoluminescence is observable and the MoS₂ Raman signal is weak because of the local field effect, that is, the local electric field at a high refractive index material like MoS₂ is much weaker than the incident electrical field. For ultrathin MoS₂ layers where local field effects are relatively small, the Raman and photoluminescence intensities show opposite layer dependence: MoS₂ Raman signal is the weakest in the monolayer MoS2 (due to reduced amount of material), while photoluminescence is the strongest in spite of the reduced amount of material. This surprising behavior of the photoluminescence indicates that luminescence quantum efficiency is much higher in MoS2 monolayer than in multilayer and in the bulk.

Next we determine layer dependent luminescence quantum efficiency η_{Lum} using an internal calibrator provided by MoS₂ Raman signal. MoS₂ Raman intensity I_{Raman} and lumi-

nescence intensity $I_{\rm Lum}$ are affected in the same manner by effects such as laser excitation intensity, quantity of material, and local electric field factors; therefore such external effects are canceled out in the ratio $I_{\rm Lum}/I_{\rm Raman}$ and this ratio provides a measure of intrinsic luminescence quantum efficiency through the quantity $\eta_{\rm Lum} \approx \eta_{\rm Raman} (I_{\rm Lum}/I_{\rm Raman})$. In this equation, we have neglected the small energy difference between luminescence and Raman scattered photons. Because Raman scattering efficiency $\eta_{\rm Raman}$ usually has little layer thickness dependence, the photoluminescence spectra normalized by Raman intensity (Figure 3b) reflects directly the luminescence efficiency $\eta_{\rm Lum}$. A dramatic jump of luminescence quantum efficiency in MoS $_2$ monolayer is evident.

The observed optical behavior in few-layer MoS2 has several unique characteristics. Bulk MoS2 does not exhibit luminescence and has strong direct excitonic absorption at energies much larger than the indirect bandgap. These excitonic states become strongly luminescent in MoS₂ monolayer, but they remain at the same transition energies as in the bulk. These characteristics are profoundly different from the behaviors reported in other low dimensional semiconductor nanostructures. Nanostructures obtained from direct bandgap semiconductors usually emit strongly upon photoexcitation, but the luminescence is present in the bulk as well. Nanostructures obtained from indirect bandgap semiconductors such as silicon show some apparent similarities to MoS2 in that silicon nanocrystals display enhanced photoluminescence compared with bulk silicon. 17 However, the underlying physics is markedly different. In silicon nanocrystals, the photoluminescence originates from quantum confined electronic states with increased emission energy at decreased nanoparticle size. More importantly, the optical transitions in silicon nanocrystals larger than \sim 2-3 nm are still indirect-gaplike with strong optical vibronic origins, 18 and the radiative transition rate remains quite low (at kHz). In addition, optical transitions in small Si nanoparticles are strongly dependent on the surface structure. 19 In contrast, MoS₂ luminescence arises from direct electronic transitions. which are allowed and thus show a much higher radiative recombination rate. Therefore no previously known mechanism in other nanostructures can account for the photoluminescence behavior in MoS₂.

The observed MoS₂ monolayer photoluminescence must be an intrinsic material property rather than due to external perturbations such as defect states, since the luminescence resonances match perfectly the direct excitonic transitions. Luminescence quantum efficiency from such direct excitonic state in MoS₂ can be approximated by $\eta_{\rm Lum} \approx k_{\rm rad}/(k_{\rm rad} + k_{\rm defect} + k_{\rm relax})$, where $k_{\rm rad}$, $k_{\rm defect}$, and $k_{\rm relax}$ are, respectively, rates of radiative recombination, defect trapping, and electron relaxation within the conduction and valence bands. Because the rate of intraband relaxation to band minimum $(k_{\rm relax})$ is extremely high, photoluminescence from direct excitonic transitions is usually not observable in indirect bandgap semiconductors. In monolayer MoS₂, $k_{\rm rad}$ is not



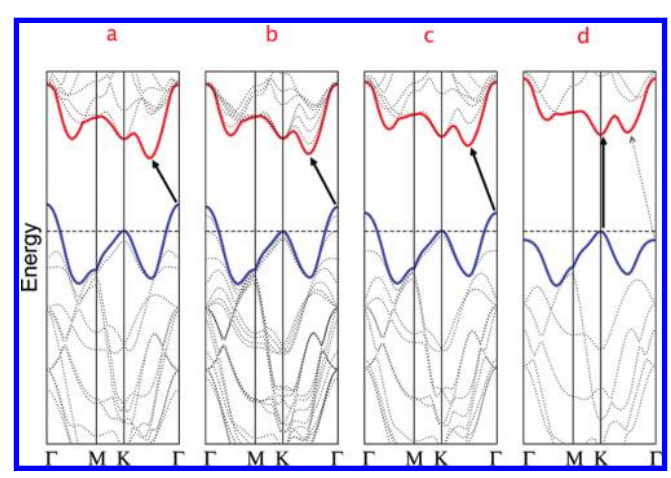


FIGURE 4. Calculated band structures of (a) bulk MoS_2 , (b) quadrilayer MoS_2 , (c) bilayer MoS_2 , and (d) monolayer MoS_2 . The solid arrows indicate the lowest energy transitions. Bulk MoS_2 is characterized by an indirect bandgap. The direct excitonic transitions occur at high energies at K point. With reduced layer thickness, the indirect bandgap becomes larger, while the direct excitonic transition barely changes. For monolayer MoS_2 in d, it becomes a direct bandgap semiconductor. This dramatic change of electronic structure in monolayer MoS_2 can explain the observed jump in monolayer photoluminescence efficiency.

likely to change appreciably with respect to bulk value, because the direct excitonic transitions remain at the same energy. Therefore, the enhanced photoluminescence in monolayer has to be attributed to a dramatically slower electronic relaxation $k_{\rm relax}$. The decrease of interband relaxation rate strongly suggests a substantial change in MoS₂ electronic structure when going from the bulk to monolayer.

Electronic structure of bulk and monolayer MoS2 has been previously investigated through ab inito calculations. 20,21 Recent theoretical results using improved algorithm and computation power predict that the indirect bandgap bulk MoS₂ becomes a direct bandgap semiconductor when thinned to a monolayer, 21 which can readily account for our experimental observations. For a detailed comparison between experiment and theory, we calculated the band structures of bulk MoS2 and ultrathin MoS2 layers with different thicknesses. We employed density functional theory with generalized gradient approximation using the PWscf package. 22 The calculation results are displayed in Figure 4. It is shown that the direct excitonic transition energy at the Brillouin zone K point barely changes with layer thickness, but the indirect bandgap increases monotonically as the number of layers decreases. Remarkably, the indirect transition energy becomes so high in monolayer MoS₂ that the material changes into a two-dimensional direct bandgap semiconductor. The variation of the electronic structure in few-layer MoS2 is in accord with our experimental data. With the increase of the indirect bandgap in thinner MoS₂, the intraband relaxation rate from the excitonic states decreases and the photoluminescence becomes stronger. In the case of monolayer MoS₂, a qualitative change into a direct bandgap semiconductor renders $k_{\rm relax}=0$, leading to a dramatic jump of luminescence that is only limited by the defect trapping rate $k_{\rm defect}$. In MoS₂ of all thicknesses, the direct excitonic transition at the K point remains at roughly the same energy.

The unusual electronic structure of few-layer MoS $_2$ and the resulting unique optical behavior stem from the characters of d-electron orbitals that comprise MoS $_2$ conduction and valence bands. Our theoretical calculations show that electronic states of different wave vectors have electron orbitals with different spatial distributions. Specifically, conduction band states at the K point are primarily composed of strongly localized d orbitals at Mo atom sites. They have minimal interlayer coupling since Mo atoms are located in the middle of the S-Mo-S unit cell. On the other hand, states near the Γ point and the point of indirect bandgap originate from a linear combination of d orbitals on Mo atoms and antibonding p_z orbitals on S atoms. They have strong interlayer coupling and their energies depend sensitively on layer thickness.

In conclusion, our study reveals a surprising emergence of photoluminescence in MoS_2 layers. This observation is consistent with the theoretical prediction of indirect to direct bandgap transition in going from multilayer to monolayer MoS_2 . Such behavior, arising from d-orbital related interactions in MoS_2 , may also arise in other layered transition metal dichalcogenides. It points out a new direction for controlling electronic structure in nanoscale materials by exploiting rich d-electron physics. Such capability can lead to engineering novel optical behaviors not found in sp-bonded materials and holds promise for new nanophotonic applications.

Acknowledgment. We thank Professor Ron Shen for helpful discussion and Professor Xiang Zhang for the AFM measurements. The work was supported by a National Science Foundation CAREER award and a Sloan fellowship (F.W.) and by DOE-BES Grant DE-FG02-06ER46262 (G.G. and T.L.). Y.Z. is supported by a Miller fellowship and A.S. acknowledges support from Scuola Galileiana di Studi Superiori di Padova and the EAP.

REFERENCES AND NOTES

- Novoselov, K. S.; Jiang, D.; Schedin, F.; Booth, T. J.; Khotkevich, V. V.; Morozov, S. V.; Geim, A. K. Proc. Natl. Acad. Sci. U.S.A. 2005, 102, 10451.
- (2) Novoselov, K. S.; Geim, A. K.; Morozov, S. V.; Jiang, D.; Katsneison, M. I.; Grigorieva, I. V.; Dubonos, S. V.; Firsov, A. A. *Nature* 2005, 438, 197.
- (3) Zhang, Y.; Tan, Y.-W.; Stormer, H. L.; Kim, P. *Nature* **2005**, *438*,
- (4) Yoffe, A. D. Adv. Phys. 2002, 51, 799.
- (5) Ayari, A.; Cobas, E.; Ogundadegbe, O.; Fuhrer, M. S. J. Appl. Phys. 2007, 101, No. 014507.
- (6) Gourmelon, E.; Lignier, O.; Hadouda, H.; Couturier, G.; Bernede, J. C.; Tedd, J.; Pouzed, J.; Salardenne, J. Sol. Energy Mater. Sol. Cells 1997, 46, 115
- Ho, W. K.; Yu, J. C.; Lin, J.; Yu, J. G.; Li, P. S. Langmuir 2004, 20, 5865.



- Frindt, R. F.; Yoffe, A. D. Proc. R. Soc. London, Ser. A 1963, 273, (8) 69.
- Frindt, R. F. Phys. Rev. 1965, 140, A536.
- (10) Lauritsen, J. V.; Kibsgaard, J.; Helveg, S.; Topsoe, H.; Clausen, B. S.; Laegsgaard, E.; Besenbacher, F. Nat. Nanotechnol. 2007, 2,
- (11)Remskar, M.; Mrzel, A.; Skraba, Z.; Jesih, A.; Ceh, M.; Demsar, J.; Stadelmann, P.; Levy, F.; Mihailovic, D. Science 2001, 292, 479.
- (12) Wieting, T. J.; Verble, J. L. Phys. Rev. B 1971, 3, 4286.
- (13) Mak, K. F.; Sfeir, M. Y.; Wu, Y.; Lui, C. H.; Misewich, J. A.; Heinz, T. F. Phys. Rev. Lett. 2008, 101, 196405.
- (14) Coehoorn, R.; Haas, C.; Dijkstra, J.; Flipse, C. J. F.; de Groot, R. A.; Wold, A. Phys. Rev. B 1987, 35, 6195.

- (15) Coehoorn, R.; Haas, C.; de Groot, R. A. Phys. Rev. B 1987, 35,
- Russell, J. P. Appl. Phys. Lett. 1965, 6, 223. (16)
- (17)Cullis, A. G.; Canham, L. T. Nature 1991, 353, 335.
- Nirmal, M.; Brus, L. Acc. Chem. Res. 1999, 32, 407.
- Godefroo, S.; Hayne, M.; Jivanescu, M.; Stesmans, A.; Zacharias, M.; Lebedev, O. L.; Tendeloo, G. V.; Moshchalkov, V. V. Nat. Nanotechnol. 2008, 3, 174.
- (20) Kobayashi, K.; Yamauchi, J. Phys. Rev. B 1995, 51, 17085.
- (21) Li, T.; Galli, G. J. Phys. Chem. C 2007, 111, 16192.
- Baroni, S.; Corso, A. D.; de Gironcoli, S.; Giannozzi, P.; Cavazzoni, C.; Ballabio, G.; Scandolo, S.; Chiarotti, G.; Focher, P.; Pasquarello, A.; Laasonen, K.; Trave, A.; Car, R.; Marzari, N.; Kokaji, A. Plane-Wave Self-Consistent Field Home Page. http://www.pwscf.org .